2016

Integral and Differential Model of Hermetical Compressor Heat Losses Including Experimental Validation

Maria Goossens
EDF R&D, Energy in Buildings and Territories Department (ENERBAT), France / Centre for Energy efficiency of Systems (CES), MINES ParisTech, PSL Research University, France, maria.niznik@mines-paristech.fr

Philippe Riviere
Centre for Energy efficiency of Systems (CES), MINES ParisTech, PSL Research University, France, philippe.riviere@mines-paristech.fr

Odile Cauret
EDF R&D, Energy in Buildings and Territories Department (ENERBAT), France, odile.cauret@edf.fr

Cedric Teuillieres
EDF R&D, Energy in Buildings and Territories Department (ENERBAT), France, cedric.teuillieres@edf.fr

Dominique Marchio
Centre for Energy efficiency of Systems (CES), MINES ParisTech, PSL Research University, France, dominique.marchio@mines-paristech.fr

Integral and Differential Model of Hermetical Compressor Heat Losses Including Experimental Validation

Maria GOOSSENS[1&2]*, Philippe RIVIERE[1], Odile CAURET[2], Cedric TEUILLIERES[2], Dominique MARCHIO[1]

[1] Mines ParisTech, PSL Research University, Centre for Energy efficiency of Systems (CES), Paris, 75006, France
Phone: +33 1 40 51 90 80, Fax: +33 1 40 51 94 49, E-mail: philippe.riviere@mines-paristech.fr

[2] EDF R&D, Energy in Buildings and Territories Department, Ecuelles, 77250, France
Phone: +33 1 60 73 67 10, E-mail: maria.goossens@edf.fr

* Corresponding Author

ABSTRACT

The current evaluation of heating and cooling system performances has become a major issue in European buildings sector. A promising method for measuring heat pump performances on-field has been previously developed and published. However, the accuracy of the method is strongly dependent on the evaluation of heat transfer from compressor towards the ambient air. In this paper a developed compressor heat transfer model that couples integral and differential formulations is presented. The model consists of three fundamental steps: thermodynamic analysis of the compression process, detailed thermophysical flow analysis using a CFD software, and finally compressor thermal network analysis consisting of integral equations that describe heat transfer of solid-fluid interfaces. Temperature distribution of the compressor shell is the main output of the model. Internal and external thermal profiles obtained from the numerical model and experimental measurements are compared in one operating condition at two compressor speeds. The RMS errors of external profiles are 3.20 °C and 1.96 °C, at 30 rps and 60 rps, respectively. The model can be used to determine the minimum number of surface temperature sensors and their locations on the compressor shell necessary to measure heat losses on-field. More accurate evaluation of compressor heat losses towards the ambient air will improve the accuracy of the performance measurement method.

1. INTRODUCTION

In an increasingly demanding regulatory setting, current methods to evaluate performances of heating and cooling systems have become problematic in European buildings sector (Ertesvag, 2011). Accurately measuring performances of air-to-air heat pumps (HPs) on-field is particularly challenging (McWilliams, 2002). A method based on mass/energy balances of the refrigeration cycle components has been adapted to measure the heat pump performances on-field (Tran *et al.*, 2013). This method integrates a simplified model of compressor heat transfer towards the ambient air, herein after referred to as the compressor heat losses. It has been established that compressor heat losses influence significantly the overall accuracy of the method: Tran *et al.* (2013) showed that the sensitivity index of the uncertainty of heating power predicted by the internal refrigerant method is 40%. Thus, a more precise evaluation of compressor heat losses is required in order to improve the HP performance analysis method.

Modeling compressor heat transfer is a challenging task. The complexity of compressor geometry hinders simplifications and contributes to various complex flow and heat transfer phenomena. Experimental and numerical approaches are typically used to model compressor thermal behavior. A short literature review in Section 2 highlights the state-of-the-art of compressor heat transfer modeling. The purpose of literature review was to aid in determining the most adequate modeling technique.

In this paper numerical model that evaluates compressor thermal behavior and heat transfer from the shell towards the ambient air is presented. Hybrid modeling approach, where differential and integral formulations are coupled, was adapted to be able to provide results with better accuracy than simply integral models, yet remaining relatively simplified, with low computational costs, and more flexible in terms of compressor design applicability, in comparison with differential models. This modeling approach is applicable to scroll and rotary compressors. Thermal behavior of scroll compressors is modeled. Thermal profiles obtained from the numerical model were compared to the ones obtained from a scroll compressor test bench. The model can be used to determine the minimum non-intrusive instrumentation, *i.e.* the minimal number of surface temperature sensors and their locations on the compressor shell, necessary to measure heat losses on-field.

2. STATE-OF-THE-ART OF COMPRESSOR HEAT TRANSFER MODELING

2.1 Correlations based on experimental measurements

Experimental techniques, where thermocouples are placed inside and/or outside the compressor, are one of the most straightforward and conventional ways to determine the thermal behavior of compressors. This approach is intrusive and the location of sensors has to be considered very carefully for the flow dynamics and the heat transfer inside the compressor to remain unaffected. Another technique is to use heat flux sensors and infrared cameras (Ribas *et al*., 2008). Experimental data gives an insight into the main heat transfer mechanisms in each internal domain of the compressor (Jang & Jeong, 2005). Furthermore, the most significant heat transfer zones between component surfaces and surrounding fluid can be quickly identified (Dutra & Deschamps, 2013).

Correlations for compressor heat losses and component thermal conductances can be derived with the acquired experimental data. Heat transfer correlations are typically functions of variables that can be measured on-field, for instance condensation temperature. The correlations can also be used in some numerical models (Diniz *et al*., 2012). However, these correlations are based on the data obtained from a limited number of operating conditions, therefore, their accuracy and overall validity is limited/unknown outside the operating range or when compressor parameters, such as the compressor layout or refrigerant type, are modified (Kim & Bullard, 2002). On the other hand, more accurate experimental models based on a great deal of operating conditions typically involve too many variables that are hard to measure on-field, such as the volumetric and isentropic efficiencies (Duprez *et al*., 2009).

2.2 Numerical models

Numerical models can be divided into three different approaches: integral, differential, and hybrid. The choice of the modeling approach depends on the desired level of complexity and applicability of the model.

Integral models consist of building a system of steady or unsteady state energy balance equations (integral formulations) for each control surface. They are often referred to as lumped conductance or thermal network (TNW) models. Control surfaces are usually limited by the geometrical boundaries of the compressor solid components. With appropriate energy balances and heat transfer coefficients the compressor components are thermally interconnected, thus forming a network. Heat transfer coefficients can be adapted from the correlations already available in literature, like in the works of Sim *et al*. (2000) and Ooi (2003). Another approach is to use experimental data to calibrate thermal conductances, such as in the model developed by Todesca *et al.* (1992). The main advantage of the integral method is its relative simplicity and flexibility to adapt to different compressor types and internal component layouts. However, the main disadvantage of this modeling approach is its poor accuracy.

Differential models solve flow equations, such as Navier-Stokes equations, for each control volume with the aid of a computational fluid dynamics (CFD) program. Such models are able to predict flow and thermal profiles in a specific compressor design (Almbauer *et al*., 2006). In the works of Chikurde *et al*. (2002), Birari *et al*. (2006), Pereira & Deschamps (2012), and Raja *et al.* (2003) steady-state thermal behavior of a hermetical reciprocating compressor is simulated, where different compressor component zones are assigned as heat sources/sinks resulting from electrical motor losses, frictional losses and heat losses due to a non-isentropic compression process. Such models provide a very accurate and detailed thermal analysis for a variety of operating conditions, and there is no need to prescribe thermal conductances. However, the developed model is usually compressor design specific. Furthermore, the computational processing time is quite high and requires powerful computers. Also, some complex physical phenomena inside the compressor, such as the flow of lubricating oil, complicate significantly the modeling strategies.

Hybrid models resolve integral and numerical formulations in a coupled manner: thermal network models are used to optimize simplified CFD models (Diniz *et al*., 2012). Thus, hybrid models are a compromise between differential and integral models, as seen in the works of Almbauer *et al.* (2006), Sanvezzo & Deschamps (2012), and Ribas (2007). Similarly to integral models, hybrid methods assign heat transfer coefficients and/or other necessary information as boundary conditions to represent the effects of the flow dynamics on the heat transfer between solid and fluid interfaces (integral formulations). This eliminates the need to create complex, computationally expensive and detailed CFD models. For instance, modeling in detail rotations and other movements of interior components and their effects on the flow and heat transfer can be avoided in the CFD geometry, mesh and setup. In this case the differential formulations resolve the evolution of flow inside the compressor and its effects on the component wall temperature with relatively low computational costs. Such models are more accurate than the integral models. Yet, they remain relatively simplified and more flexible in terms of compressor design applicability in comparison with differential models (Ribas et al., 2008). Heat transfer from compressor shell towards ambient air was not a primary interest of the hybrid models found in literature. Also, most hybrid models consider reciprocating compressors. Diniz *et al.* (2012) developed a hybrid thermal model for scroll compressors. However, the model integrates temperature distribution along the scroll wraps; thus, it is adapted only for scroll compressors.

3. COMPRESSOR HEAT LOSS MODEL

Figure 1 is a schematic representation of the computational domain for scroll compressors. The model is simplified by removing unnecessary fillets and parts in order to facilitate the meshing in the preprocessing stage and the convergence in CFD solver. Compressor is surrounded by ambient air with enclosure walls maintained at a constant temperature. Depending on the configuration compressor shell can either be exposed to forced or natural convection. The geometrical domain consists of compression chamber, crankshaft, compressor shell, oil sump at the bottom, rotor, and stator. The listed components were considered as the most essential from the heat transfer point of view.

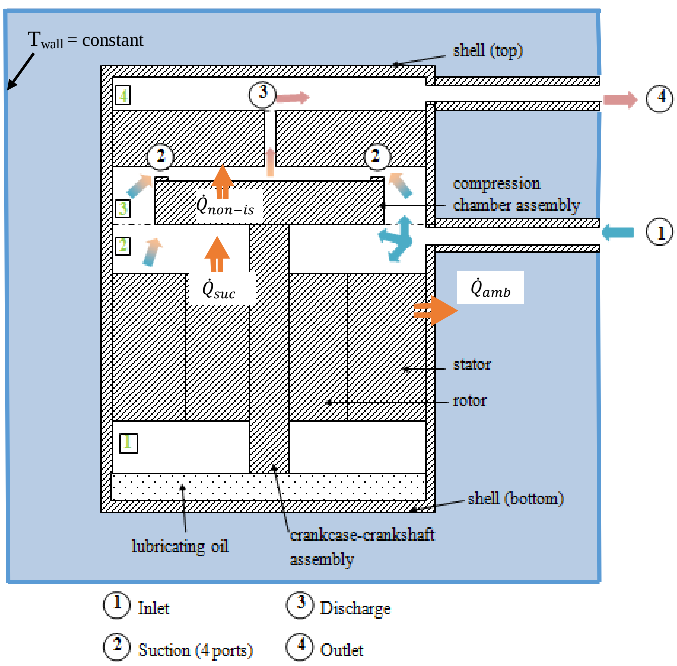

Figure 1. Schematic of the scroll compressor domain

The calculation procedure can be divided into three fundamental steps: thermodynamic cycle analysis, detailed thermophysical flow analysis, and compressor thermal network analysis, as depicted in Figure 2.

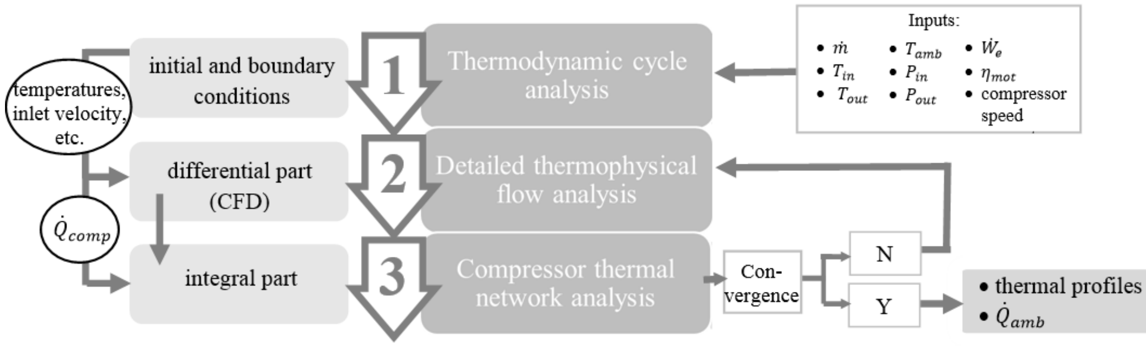

Figure 2. Schematic of the model calculation steps

3.1 Thermodynamic cycle analysis

The first part of the model analyzes the thermodynamic compression cycle in order to evaluate the initial and boundary conditions, such as temperatures, inlet velocity, and heat sources, used in integral and differential parts of the model, steps two and three, respectively. In this part heat released by the compression process is calculated. This variable is used in the third step of the model to determine whether the model has converged.

It is assumed that the heat released by the components, $\dot{Q}_{comp}$, is partially absorbed by the fluid and partially transmitted towards the ambient air, and can be calculated from Equation (1):

$$\dot{Q}_{comp} = \dot{Q}_{suc} + \dot{Q}_{non-is} \tag{1}$$

where $\dot{Q}_{suc}$ is the superheat of the refrigerant gas passing from the compressor inlet to the compression chamber, and $\dot{Q}_{non-is}$ is the heat released due to a non-isentropic compression process. Gas superheat is assumed to be equal to electrical losses dissipated as heat from the motor, located at the bottom of the hermetical compressor (Figure 1), given in Equation (2):

$$\dot{Q}_{suc} = (1-\eta_{mot})\dot{W}_e \tag{2}$$

where η_{mot} is the motor efficiency and $\dot{W}_e$ electrical power consumption. In order to calculate $\dot{Q}_{non-is}$, the isentropic compression power, given in Equation (3), must be known:

$$\dot{W}_{is} = \dot{m}\left(h_{dis,is} - h_{suc}\right) \tag{3}$$

where $\dot{m}$ is the mass flow rate of the fluid, h_{suc} is the refrigerant enthalpy at the suction chamber cavity, and $h_{dis,is}$ is the discharge enthalpy of an isentropic compression determined from Equation (4):

$$h_{dis} = h\left(s\left(T_{suc}, P_{in}\right), P_{dis}\right) \tag{4}$$

where P_{dis} is the discharge pressure and $s(T_{suc}, P_{in})$ is the fluid entropy at the suction chamber cavity. Consequently, $\dot{Q}_{non-is}$ is obtained from Equation (5):

$$\dot{Q}_{non-is} = \eta_{mot}\dot{W}_e - \dot{W}_{is} \, . \tag{5}$$

Figure 3 illustrates the thermodynamic cycle of heat pumps and associated power distribution. This step is coded in a computational code, MATLAB. The required refrigerant gas properties, such as enthalpies, are obtained from the libraries of REFPROP (NIST, 2008).

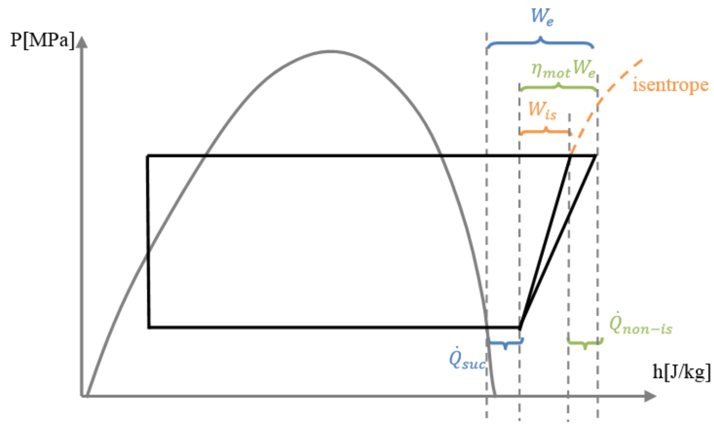

Figure 3. Thermodynamic refrigeration cycle of a heat pump

3.2 Detailed thermophysical flow analysis

The second step of the model is executed in ANSYS FLUENT, a CFD code that numerically solves a set of governing differential equations (conservation of mass, momentum and energy). The outcomes of this part of the model are refrigerant thermal and flow profiles, as well as solid zone temperatures. This information is subsequently transmitted to the final step of the model in order to perform a TNW analysis that verifies the CFD simulation results.

The domain geometry of the CFD model is decomposed into solid and fluid zones. The sub domains are oil continuum (on the bottom of the compressor cylinder), discrete refrigerant fluid zones, surrounding air continuum, and solid zones bounded by simplified geometrical boundaries of the components. The domain mesh consists of $3.40 \cdot 10^6$ tetrahedral elements. Denser mesh is imposed in narrow passages and regions with more significant curvature. Steady state, conduction between solid-solid and convection and radiation between fluid-solid interfaces is enabled in the domain. The solver type is segregated and pressure-based. Gravitational acceleration is enabled in the domain. Standard k-epsilon model, was chosen as the turbulence model for its robustness, economy, and reasonable accuracy. Velocity inlet and outflow were set at the inlet and outlet boundary conditions, respectively. The walls of the air enclosure surrounding the compressor are isothermal. Boussinesq approximation was applied for the air density. Volumetric and surface heat fluxes were added to the computational domain.

The CFD model performs exclusively a thermal analysis and, therefore, no compression is assumed to take place in this part of the model. To represent an increase in temperature from T_{suc} to T_{dis}, temperatures of the refrigerant at suction and discharge, respectively, due to compression and non-isentropic heat, a heat flux is introduced in the compression chamber, $\dot{Q}_{comp-cham}$ (Figure 4). Oil sump and top of the crankshaft temperatures are set as constant and calculated from a multivariate correlation for oil temperature. The correlation was derived from experimental data over a range of operating conditions, where the difference between condensation and evaporation temperatures varied from 25 to 60 °C. Also, multiple compressor speeds and ambient temperatures were considered.

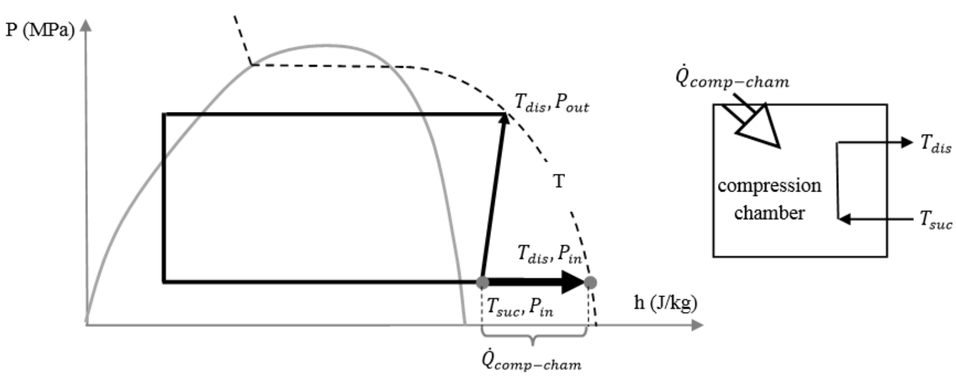

Figure 4. Required heat to reach $\boldsymbol{T_{dis}}$ (temperature of the compressed fluid at discharge)

3.3 Compressor thermal network analysis

The final step of the model involves a network of energy transfer equations between the solid-fluid interfaces by convection. The goal of the TNW analysis is to verify that the heat, $\dot{Q}_{comp}$, calculated from Equation (1), equals to the heat dissipated from compressor components, as listed in Equation (6):

$$\dot{Q}_{comp} = \dot{Q}_{rotor} + \dot{Q}_{stator} + \dot{Q}_{crank} + \dot{Q}_{comp-cham} \tag{6}$$

The total heat flux of each component is the sum of all heat fluxes of individual surfaces that constitute the component in question. For instance, heat transferred from the rotor to the surroundings is the sum of heat fluxes between the fluid and rotor surface in contact with the fluid. If the heat released due to an imperfect compression process, $\dot{Q}_{comp}$, obtained from Equation (1), is equal to the heat released by the compressor components, obtained from Equation (6), the model converged. If not, more boundary conditions may be assigned in CFD model to guide the differential step more effectively, until convergence is achieved.

In order to obtain the net energy released by the components, the temperatures of the solid components and surrounding fluid, as well as the refrigerant velocities in proximity to the solid components must be known. These values are obtained from the CFD model. Consequently, convective heat transfer coefficients are evaluated. Nusselt number correlations for different flow regimes and geometries were taken from literature. Correlations for internal and external flows for horizontal and vertical, rotating and static plates and cylinders were considered. Equation (7) describes the relation between the Nusselt number and the convective heat transfer coefficient:

$$Nu_x = h_x x / k \tag{7}$$

where x is the characteristic length, which depending on the geometry of the object and flow characteristics can be a diameter, radius or length, k is the thermal conductivity of the fluid, and h_x is the convective heat transfer coefficient (Incropera, 2002).

As the convergence in step three is achieved, $\dot{Q}_{amb}$ values are extracted directly from the CFD model. Numerical results of $\dot{Q}_{amb}$ presented in Table 1 were obtained at T_{cond}=60 °C, T_{evap}=0 °C, and T_{amb}=10 °C at two compressor speeds, 30 rps and 60 rps, with R407C as the refrigerant fluid.

Table 1. Numerical results of $\dot{\boldsymbol{Q}}_{\boldsymbol{amb}}$ expressed as a percentage of compressor power input at different speeds

Speed (rps)	Numerical (%)
30	10.84
60	7.36

This part established the hybrid model. The results in Table 1 are expressed in percentages for confidentiality reasons. The second step (CFD model) took approximately 4 hours to converge, and for the third step to converge, the value obtained in Equation (6) had to fall within the ±10% range of the value obtained from Equation (1).

4. EXPERIMENTAL COMPARISON

Numerical results were compared to experimental values obtained from a scroll compressor test bench. Compressor component layout was identical to the one of the numerical model (Figure 1). Air temperature in the climate chamber was maintained at 10 °C, and the evaporation and condensation temperatures were 0 °C and 60 °C, respectively, at 30 rps and 60 rps. The tested compressor had no insulation, and R407C was used as the refrigerant fluid. In the experimental setup 40 thermocouples were placed along the compressor shell and on the internal components, such as the motor and discharge baffle. Refrigerant mass flow rate, oil concentration in the refrigerant circuit, compressor inlet and outlet temperatures, condensation and evaporation pressures, and compressor power input were also measured. All values were registered in steady operating state, about 10 minutes after start up. Experimental values of compressor heat losses were calculated from the compressor energy balance equation given in Equation (8):

$$\dot{Q}_{amb} = \dot{W}_{comp} - \dot{m}\left[\left(1-C_g\right)\left(h_{r,comp,out} - h_{r,comp,in}\right) + C_g \Delta h_o^{T_{comp,in} \to T_{comp,out}}\right] \tag{8}$$

where $h_{r,comp,out}$ and $h_{r,comp,in}$ are the refrigerant enthalpies at compressor inlet and outlet, respectively, $\dot{W}_{comp}$ is the compressor power input, $\Delta h_o^{T_{comp,in} \to T_{comp,out}}$ is the enthalpy change of oil, and C_g is the oil mass fraction. Error propagation formula, listed in Equation (9), was used to evaluate the absolute error of experimental heat losses:

$$\sigma_{\dot{Q}_{amb}} = \sqrt{\sum_i \left(\frac{\delta \dot{Q}_{amb}}{\delta n_i}\right)^2 \sigma_{n_i}^2} \tag{9}$$

where n_i is the measured variable, and σ_{n_i} is the absolute uncertainty of the measured quantity. Wattmeter, flow meter, pressure sensor, and surface temperature sensor uncertainties were taken into consideration.

In Figure 5, numerical and experimental temperatures, expressed in dimensionless values for confidentiality reasons, distributed along the exterior compressor shell are compared at two compressor speeds. Measuring points 1-7 represent the locations of thermocouples along the shell, from the bottom to the top. The RMS errors of external profiles are 3.20 °C and 1.96 °C, at 30 rps and 60 rps, respectively. Numerical and experimental temperature values of the internal components are compared in Figure 6. Compressor heat losses obtained from the numerical model and experimental tests are presented in Table 2.

In hermetical compressors lubricating oil prevents potential damage of internal components due to friction. In addition to oil being stored in the sump at the bottom, a thin oil film is present over many components inside the compressor, such as the crankcase, stator and the internal surface of the compressor shell. The oil pump is coupled with the crankshaft; as the shaft spins, the lubricating oil flows inside the pump through the crankshaft by centrifugal forces. As it reaches the other extremity of the shaft assembly, part of it is projected as a jet hitting the upper surface of the compressor shell along which it later flows as a thin oil film. The other part of the projected oil returns to the sump by flowing over the compressor crankcase. Oil forms an interface between the refrigerant fluid and the surface of the solid components. Thus, it can affect the heat transfer inside the compressor (Dutra & Deschamps, 2013). In the numerical model, oil is still and present only at the bottom. This could be the reason for the discrepancies between the experimental and numerical results.

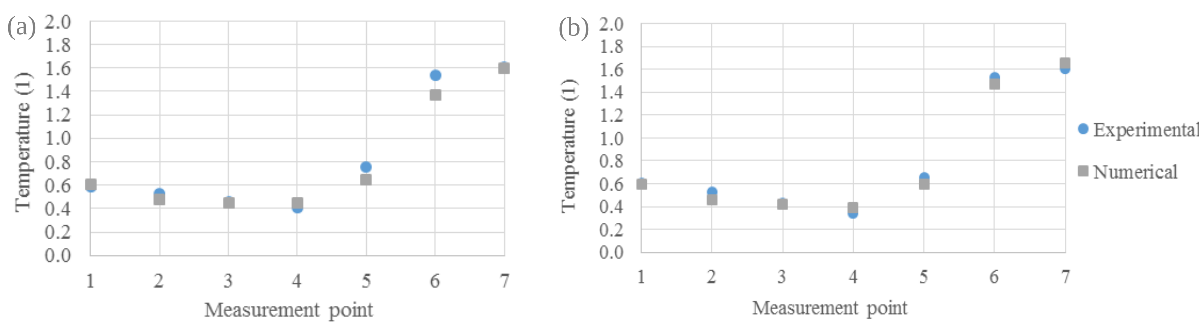

Figure 5. Shell temperature distribution (dimensionless values) at 30 rps (a) and 60 rps (b)

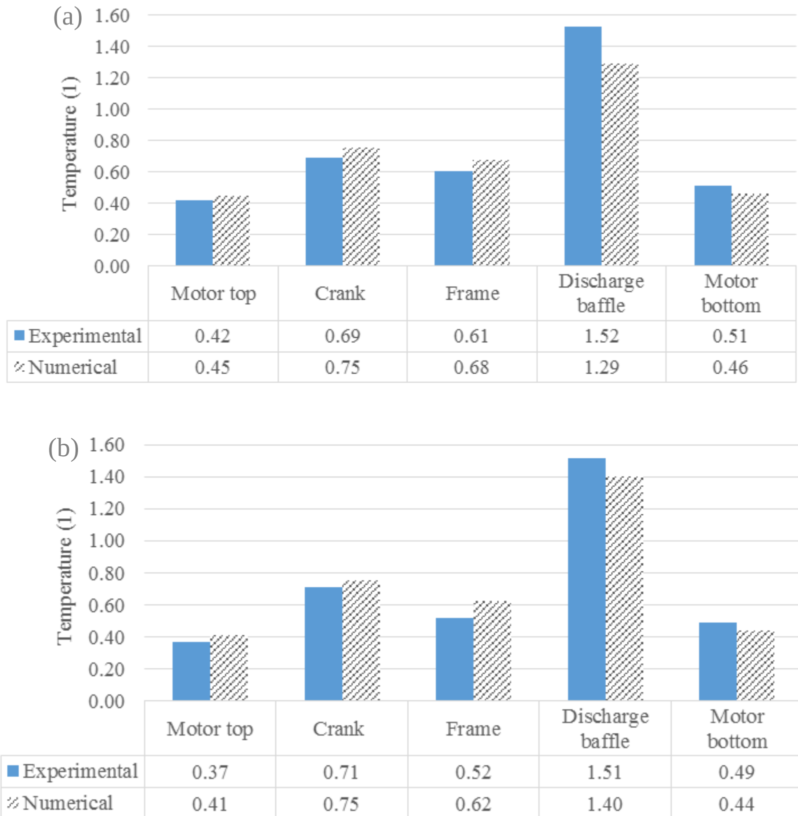

Figure 6. Dimensionless temperature values of internal compressor components at 30 rps (a) and 60 rps (b)

Table 2. Experimental and numerical $\dot{\boldsymbol{Q}}_{\boldsymbol{amb}}$ values expressed as a percentage of compressor power input

Speed (rps)	Experimental (%)	Numerical (%)
30	11.48±1.71	10.84
60	8.31±1.78	7.36

5. CONCLUSIONS

A numerical model used to determine the temperature distribution of the compressor exterior shell was developed. A code was written in a computing language representing the thermal network of the compressor, which is coupled with a commercially available CFD code that solves differential equations in order to perform a more elaborate flow and heat transfer analysis in the compressor domain. Model outputs are compared with experimental results obtained from a hermetical scroll compressor that has been accurately instrumented and tested in a compressor test bench. Internal and external thermal profiles are compared in one operating condition at two different speeds. The RMS errors of the shell temperatures at different locations are 3.20 °C and 1.96 °C at compressor speeds of 30 rps and 60 rps, respectively. Compressor heat losses calculated from the compressor energy balance using the measured data were compared with the heat losses obtained from the numerical model. Numerical model can be used to determine the locations of surface temperature sensors used to evaluate heat losses of scroll compressors on-field.

NOMENCLATURE

C_g	oil mass concentration	(-)
h	specific enthalpy	(J kg^{-1})
h	heat transfer coefficient	(W m^{-2} °C^{-1})
k	thermal conductivity	(W m^{-1} °C^{-1})
m	number of thermal zones	(-)

$\dot{m}$	mass flow rate	(kg s^{-1})
n	measured variable	(-)
Nu	Nusselt number	(-)
P	pressure	(Mpa)
$\dot{Q}$	heating power	(W)
s	specific entropy	(J kg^{-1} $°C^{-1}$)
T	temperature	(°C)
UA	thermal conductance	(W $°C^{-1}$)
$\dot{W}$	power consumption	(W)
x	characteristic length	(m)
η_{mot}	motor efficiency	(-)
σ	standard deviation	(-)

Subscript

in	inlet
out	outlet
comp	component
comp-cham	compression chamber
amb	ambient
suc	suction
non-is	non-isentropic
e	electric
dis	discharge
is	isentropic
o	oil
r	refrigerant

Abbreviations

CFD	computational fluid dynamics
HP	heat pump
RMS	root-mean-square
R407C	refrigerant type
TNW	thermal network

REFERENCES

Almbauer, R. A., Burgstaller, A., Abidin, Z., & Nagy, D. (2006). 3-Dimensional simulation for obtaining the heat transfer correlations of a thermal network calculation for a hermetic reciprocating compressor. *Proc. of the Int. Compressor Engineering Conference at Purdue*, Paper C079.

Birari, Y. V., Gosavi, S. S., & Jorwekar, P. P. (2006). Use of CFD in design and developement of R404a reciprocating compressor. *Proc. of the Int. Compressor Engineering Conference at Purdue*, Paper C072.

Chikurde, R. C., Loganathan, E., Dandekar, D. P., & Manivasagam, S. (2002). Thermal mapping of hermetically sealed compressors using computational fluid dynamics. *Proc. of the Int. Compressor Engineering Conference at Purdue*, Paper C6-4.

Diniz, M. C., Pereira, E. L., & Deschamps, C. J. (2012). A lumped-parameter thermal model for scroll compressors including the solution for the temperature distribution along the scroll wraps. *Int. J. Refrig.*, *53*(2015), 184-194.

Duprez, M.-E., Dumont, E., & Frère, M. (2009). Modeling of scroll compressors - Improvements. *Int. J. Refrig.*, *33*(4), 721-728.

Dutra, T., & Deschamps, C. J. (2013). Experimental characterization of heat transfer in the components of a small hermetic reciprocating compressor. *Appl. Therm. Eng.*, *58*(1-2), 499-510.

Ertesvag, I. S. (2011). Uncertainties in heat-pump coefficient of performance (COP) and exergy efficiency based on standardized testing, *Energy and Buildings*, *43*, 1937-1946.

Incropera, F. P. (2002). *Fundamentals of heat and mass transfer*. New York, USA: John Wiley & Sons.

Jang, K., & Jeong, S. (2005). Experimental investigation on convective heat transfer mechanism in a scroll compressor. *Int. J. Refrig.*, *29*(5), 744-753.

Kim, M.-H., & Bullard, C. W. (2002). Thermal performance analysis of small hermetic refrigeration and air-conditioning compressors. *JSME International Journal*, *45*(4), 857-864.
McWilliams, J. (2002). *Review of Airflow Measurement Techniques*. Contract for U.S. Department of Energy, Contract No. DEAC03e76SF00098
NIST, National Institute of Standards and Technology (2008). *Refprop – Reference Fluid Thermodynamic and Transport Properties*, vol. 8. USA.
Ooi, K. T. (2003). Heat transfer study of a hermetic refrigeration compressor. *Appl. Therm. Eng.*, *23*(15), 1931-1945.
Pereira, E. L., & Deschamps, C. J. (2012). A numerical study of convective heat transfer in the compression chambers of scroll compressors. *Proc. of the Int. Compressor Engineering Conference at Purdue*, Paper 1274.
Pizarro-Recabarren, R. (2009). Modelling the influence of the lubricant oil on the heat transfer in hermetic reciprocating compressor. *Proc. of the Int. Conference on Compressors and Their Systems* (365-374). London.
Raja, B., J., Sekhar. S. J., Lal, D. M., & Kalanidhi, A. (2003). A numerical model for thermal mapping in a hermetically sealed reciprocating refrigerant compressor. *Int. J. Refrig*., *26*(6), 652-658.
Ribas, F. A. (2007). Thermal analysis of reciprocating compressors. *Proc. of Int. Conference on Compressor and Their Systems* (227-287). London.
Ribas, F. A., Deschamps, C. J., Fagotti, F., Morriesen, A., & Dutra, T. (2008). Thermal analysis of reciprocating compressors - critical review. *Proc. of the Int. Compressor Engineering Conference at Purdue*, Paper 1306.
Sanvezzo, J., & Deschamps, C. J. (2012). A heat transfer model combining differential and integral formulations for thermal analysis of reciprocating compressors. *Proc. of the Int. Compressor Engineering Conference at Purdue*, Paper 1343.
Sim, Y. H., Youn, Y., & Min, M. K. (2000). A study on heat transfer and performance analysis of hermetic reciprocating compressors for refrigerators. *Proc. of the Int. Compressor Engineering Conference at Purdue*, (229-236).
Todesca, M. L., Fagotti, F., Prata, A. T., & Ferreira, R. T. (1992). Thermal energy analysis in reciprocating hermetic compressors. *Proc. of the Int. Compressor Engineering Conference at Purdue* (1417-1428).
Tran, C. T., Rivière, P., Marchio, D., & Arzano-Daurelle, C. (2013), In situ measurement methods of air to air heat pump performance. *Int. J. Refrig. 35*(5), 1442-1455.
White, F. (2005). *Viscous Fluid Flow*. New York, USA: McGraw-Hill Science.

ACKNOWLEDGEMENT

The authors would like to thank Mitsubishi Heavy Industries (MHI) for providing experimental data from conducted compressor tests. This study was also made possible with the means provided by EDF R&D and Centre for Energy efficiency of Systems (CES) of Mines ParisTech.